Received: 31 January 2022 | Revised: 31 July 2022 | Accepted: 12 September 2022

DOI: 10.1002/cjce.24708

SPECIAL ISSUE ARTICLE

THE CANADIAN JOURNAL OF CHEMICAL ENGINEERING

Fuel properties and combustion performance of hydrochars prepared by hydrothermal carbonization of different recycling paper mill wastes

Englatina I. N. C. Assis | **Evans M. N. Chirwa**

Department of Chemical Engineering, Water Utilisation and Environmental Engineering Division, University of Pretoria, Pretoria, South Africa

Correspondence
Englatina I. N. C. Assis, Department of Chemical Engineering, Water Utilisation and Environmental Engineering Division, University of Pretoria, Pretoria, 0002, South Africa.
Email: englatina.assis@gmail.com

Funding information
National Research Foundation, Grant/Award Numbers: CSUR210111581519, EQP210111581520, IFR200206501999; Rand Water Chair in Water Utilisation; Sedibeng Water Chair in Water Utilisation Engineering, Grant/Award Number: 4540105923

Abstract

The incineration of high-moisture solid residues generated at the recycling paper mills represents an energetically unfavourable method of resource utilization. Alternatively, hydrothermal pre-treatment is considered. In this study, low-value paper sludges from three different recycling streams were hydrothermally carbonized at 205, 225, and 245°C for 3 h. The raw feedstocks and derived hydrochars were analyzed for energy properties, chemical characteristics, surface morphology, functional groups, and combustion performance employing energy densification and mass yield quantification, scanning electron microscopy, elemental analyzer, Fourier-transform infrared spectroscopy, and thermogravimetry. The increase in reaction temperature was reported to cause a decrease in mass yield and an increase in energy densification and calorific values corresponding to 5.98%–49.35% and 10.10%–58.51% for raw fibre rejects and final sludge-derived hydrochar, respectively. Hydrothermal carbonization (HTC) had a non-significant influence on the energy densification of primary clarifier sludge-derived hydrochar. Higher reaction temperatures favoured the rate of dehydration and decarboxylation, leading to hydrochars with lower H/C and O/C ratios, thereby enhancing the overall fuel properties. The low-nitrogen and low-sulphur fuels obtained validated the effectiveness of HTC treatment to produce high-quality cleaner solid fuel. The burnout temperature was mostly reduced with an increase in HTC temperature. At HTC-205 and 225°C, the ignition temperature and the combustion performance increased as a result of the HTC reaction mechanisms. HTC effectively recovered hydrochar with increased carbon content, improved energy densification, and good combustion adequacy. Hydrochar derived from recycling mills may play a role in the energy sector as a substitute for coal or in co-combustion at coal-fired power plants.

KEYWORDS
combustion, hydrochar, hydrothermal carbonization, ignition temperature, paper sludge

1 | INTRODUCTION

South Africa is the largest consumer of energy in the African continent[1] and the 7th largest producer of coal.[2,3] Coal represents the largest source of energy in South Africa. About 91% of the electricity nationwide is generated through coal combustion in steam-driven power plants.[4] Although coal mining and application have successfully contributed to electricity generation, these activities have an adverse effect on the environment, particularly, land, water, and air due to the substantial emission of CO_2 annually,[3] thereby placing the country in the top 10 greenhouse gas emitters in the world.[5] To reduce the environmental degradation from over-dependence on coal, the government adopted enabling policies and frameworks for the development of renewable energy resources, including solar, wind, biomass, geothermal, hydropower, waste to energy, and tidal, or wave energy.[3] The implementation of renewable energy resources can significantly reduce the overreliance on coal, decrease environmental emissions, and diversify employment opportunities, which has a positive impact on the economy.

Sludge is an undesired and inevitable by-product of the paper manufacturing process and is generated in large quantities every year.[6] On a moisture-free basis, sludge is mostly composed of carbon in the form of lignocellulose,[7] which is an excellent renewable energy source. Generally, recycling paper mills are known to generate a substantial amount of waste residues in comparison to mills that employ virgin wood, especially when paper grades such as tissue, newsprint, unbleached, and printing and writing are manufactured, where the quantity of waste generated normally ranges between 12 and 406 kg/ton.[8] This is partially associated with fillers in the paper (clay or calcium carbonate), which make the fibres inadequate for paper production.[8] Among the disposal alternatives, incineration is the most frequently used. The technique involves combusting sludge at high temperatures to generate power through steam turbines, which reduces the waste volume by up to 90%[9] while still meeting steam demand. However, the presence of high moisture and low carbon content in the form of lignocellulosic matter makes the incineration process energetically unfavourable, as each 1% moisture present in the sludge requires a 10°C increase in combustion temperature.[10] Due to these shortcomings, the current management and disposal practices of paper sludge are associated with economic, environmental, and social costs, which are likely to increase over time. Thus, economically and environmentally accepted disposal procedures should be explored.

Hydrothermal carbonization (HTC) was first introduced by Friederich Bergius in 1913 to mimic the natural process of coal formation that converted cellulose into coal-like materials.[11,12] However, until the last decade, its application to the upgrading of diverse biomass and waste feedstocks received little attention. Hydrothermal treatment has recently been rediscovered as an essential technique for the production of a variety of carbonaceous solid products, by means of CO_2 sequestration, soil quality upgradation, and energy source.[13–18] HTC is a good approach to upgrade wet, low-value fuels by increasing their respective energy density, decreasing oxygen and volatile contents and enhancing hydrophobic properties,[12,18] particularly, sludge, a low-cost moisture-rich feedstock. The conversion of sludge to solid hydrochar increases the potential for energetic applications and provides significant ease in handling, storage, and transportation.[19] HTC offers advantages over dry thermochemical processes such as pyrolysis, torrefaction, and gasification, as the process is not influenced by the moisture content of the feedstock,[20] it requires subcritical to supercritical water temperatures under autogenous pressure,[21–24] which is relatively low, and the overall process is considered exothermic,[25] thereby decreasing the energy consumption. Moreover, the resulting solid product known as 'hydrochar' has higher energy density[26] with cleaner properties[27] compared to the raw feedstock, is easily dewatered, and can be applied in mono-combustion or co-combustion at coal-fired power plants for electricity generation.

The HTC process is governed by temperature, residence time, feedstock composition, pH, and system pressure.[12,28] During HTC, an increase in temperature is associated with an increase in carbon content in the solid phase and a subsequent decrease in the solid yield[29,30] due to the significant degradation of cellulose and partial degradation of lignin at higher temperatures, while at low temperatures, mostly hemicellulose participates in the reaction.[31] Residence time plays an important role as it affects the process's thermal energy consumption. The residence time for an HTC process typically ranges from a few minutes to several hours.[32,33] Longer residence time improves dehydration and decarboxylation reactions and favours the formation of water-soluble compounds.[28,34] Feedstock composition, that is, low carbon and high ash, results in hydrochar with poor quality.[35] Acidic conditions are known to catalyze the carbonization of biomass by facilitating the hydrolysis of cellulose.[28] Pressure is self-generating and increases autogenously during the HTC and is mainly considered an indirect parameter since the HTC process is primarily dependent on temperature. The increase in pressure results in easier dissolution of

the water-extractable present in biomass, however, high pressures weaken dehydration and decarboxylation reactions.[28]

Recent studies have focused on the effect of HTC process variables on the physicochemical properties and combustion parameters of hydrochar formation from biomass, animal waste, agricultural wastes, and municipal wastewater semisolids[21,22,24,36] to elucidate the mechanisms involved in the conversion of such wastes during the HTC process. Liang et al.[21] investigated the HTC reaction mechanisms and combustion performance of hydrochar derived from forest waste and observed that higher reaction severity favoured mainly dehydration and decarboxylation reactions, which in turn led to low hydrochar yield with enhanced morphology, that is, increased surface area, pore volume, and average pore diameter as a result of lower volatile content compared to the feedstock. In addition to different carbonaceous structures, the produced hydrochar presented lower sulphur, decreased ash content, and a more stable structure, which contributed to its enhanced combustion compared to the initial substrate. Lang et al.[22] studied the effect of HTC temperatures (180–220°C) on the properties of hydrochar derived from cattle manure and further investigated the effect of the variation of heating rate (10–40°C/min) on the combustion performance and kinetic parameters of the derived hydrochar. They reported hydrochars with a significant increase in carbon composition, fixed carbon, and calorific value (about 19%, 58%, and 21%, respectively), a gradual decrease in ignition temperature at higher reaction severity, and improved combustion performances as a result of lower volatiles. Furthermore, the variation in the heating rate had no significant effect on the combustion performance of the raw feedstock and derived hydrochars. Li et al.[24] reported red jujube branch hydrochar with an amorphous structure with decreased burnout and combustion temperature and higher reaction severities.

There is limited research elucidating the mechanism involved in the combustion parameters of hydrochar prepared from different paper mill waste sources. Thus, this study aims to evaluate the hydrothermal decomposition temperature (205–245°C) of paper mill sludge from three different recycling mills streams to clarify the conversion mechanisms and the effects on the physicochemical characteristics of the produced hydrochar in comparison to the feedstocks and to further investigate the parameters involved in the combustion of the derived hydrochars and their initial substrates. Based on the evaluation, the results were reported to provide reference for extensive application of paper mill wastes as a renewable energy resource.

2 | MATERIALS AND METHODS

2.1 | Raw material

Three different substrates were subjected to HTC treatment; namely, raw fibre rejects (RF) collected from the repulping process, sludge generated at the primary clarifier (primary sludge [PS]) during physicochemical treatment of the raw wastewater from the paper mill, and final waste sludge (FS) generated from the raw wastewater, consisting of 21.1%, 23.4%, and 14.3, respectively. RF and PS were collected from a mill that uses a combination of both recycled and virgin fibre, while FS was collected from a mill that processes paper as feedstock. The samples were dewatered on-site and collected on an air-dried basis.

2.2 | Hydrochar preparation

About 10 g sample was mixed with 90 ml deionized water and hydrothermally carbonized at 205, 225, and 245°C for 3 h, according to the procedures previously reported.[35] The temperature range and reaction time were selected to ensure sufficient degradation of hemicellulose and cellulose polymers[12,34] while maintaining the degradation of lignin at a minimum, to achieve hydrochar with the lowest possible volatile content and maximum fixed carbon increase.[37] A schematic diagram involving all the tests reported in this study is illustrated in Figure 1. The hydrochar yield (H_y) was determined according to the following equation:

$$H_y\ (\%) = \frac{\mathrm{Wt}_{H(\mathrm{d.b.})}}{\mathrm{Wt}_f(\mathrm{d.b.})} \times 100 \quad (1)$$

where Wt_H and Wt_f represent the mass of dried hydrochar and the mass of dried raw sludge, respectively.

The raw feedstock and dried hydrochar samples were pulverized using a mortar and pestle and sieved to a particle size of less than 250 μm for further characterization.

2.3 | Feedstock and hydrochars characterization

Elements on the surface of the raw samples were analyzed following scanning electron microscopy by energy-dispersed X-ray spectroscopy (EDS) (Zeiss Gemini 2 Crossbeam 540 FEG-SEM with EDS & BS detector, Oxford Instruments) using a microanalysis software (Aztec 3.0 SP1). The working distance was 8.3–8.8 mm, and the target voltage (EHT) of 20 kV.

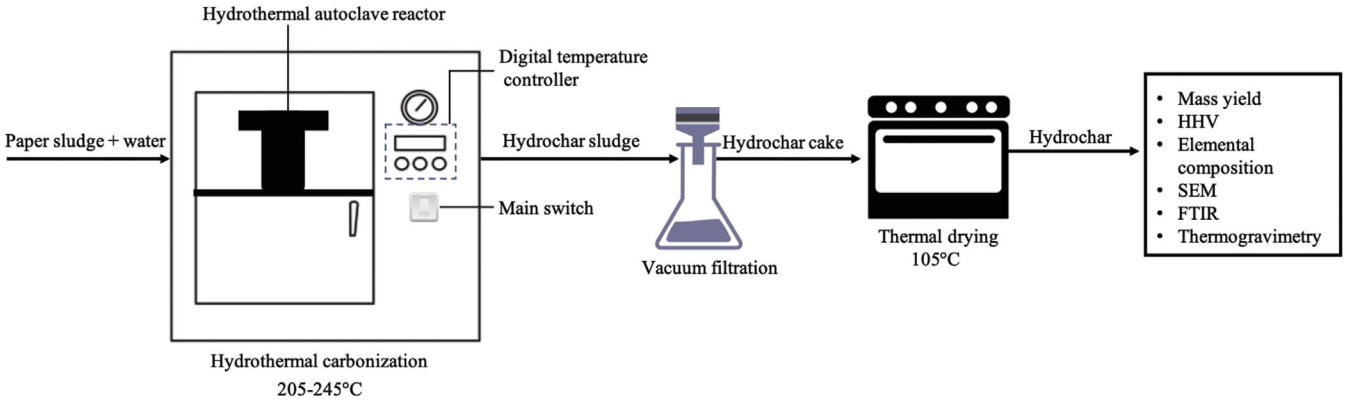

FIGURE 1 Schematic diagram of experimental procedure

The elemental CHNS composition of the samples was assessed using a Flash 2000 Elemental analyzer (Thermo Fisher Scientific) at an external laboratory, according to the method described by Kirmse.[38] The oxygen weight percentage was estimated according to Equation (2).

$$\mathrm{O}\ (\%) = 100 - (\mathrm{C} + \mathrm{H} + \mathrm{N} + \mathrm{S}) \tag{2}$$

The calorific values by means of higher heating value (HHV) were determined using a bomb calorimeter (Parr 6200 Oxygen Bomb Calorimeter) according to ASTM D5865-19. The energy densification (E_d) was calculated according to Equation (3).

$$E_{\mathrm{d}} = \frac{\mathrm{HHV}_H}{\mathrm{HHV}_f} \times 100 \tag{3}$$

where HHV_H and HHV_f represent the HHVs of the hydrochar and raw feedstock, MJ/kg.

The energy remaining in the hydrochar compared to its raw feedstock, also referred to as energy yield (E_y), was calculated using Equation (4).

$$E_{\mathrm{y}}(\%) = E_{\mathrm{d}} \times H_{\mathrm{y}}(\%) \tag{4}$$

The surface morphology of hydrochars was examined on a Zeiss Gemini 2 Crossbeam 540 field emission gun scanning electron microscope (FEG-SEM) according to Assis and Chirwa.[39] The imaging was conducted at 5 k, a working distance of 3.6–3.8 mm and a magnification of 3000 times.

Fourier-transform infrared spectroscopy (FTIR) investigation was conducted to further understand the functional groups on the surface of the raw substrates and the produced hydrochars. The analyses were performed on a PerkinElmer 100 Spectrometer. The transmission spectra were recorded in the range of 4000–550 cm^{-1}, resolution of 4 cm^{-1} by averaging 32 scans.

2.4 | Combustion performance analysis

2.4.1 | Thermogravimetric (TG) analysis

Combustion experiments were carried out in a TG analyzer (Hitachi STA300 TGA-DTA). Approximately, 10 mg of each sample was placed in a crucible and heated to 950°C at a flow rate of 80 ml/min under an air environment, followed by a 10-min isothermal hold. The weight loss and the corresponding weight loss rate (derivative thermogravimetry [DTG]) of the samples were measured continuously under the non-isothermal condition at a constant heating rate of 20°C/min.

The ignition temperature (T_i), maximum combustion rate temperature (T_m), and the burnout temperature (T_b), as well as the corresponding time, were recorded from the TG-DTG curves using the intersection method (IM) as described by Lu and Chen.[40]

2.4.2 | Calculation of combustion parameters

For further evaluation of the combustion ability and performances of the samples, the ignition index (D_i) and the comprehensive combustibility index (S) were estimated using Equations (5) and (6).

$$D_{\mathrm{i}} = \frac{\left(\frac{\mathrm{dm}}{\mathrm{dt}}\right)_{\max}}{t_{\max} \times t_{\mathrm{i}}} \tag{5}$$

where t_{max} is the time corresponding to the maximum combustion rate (min), and t_i is the ignition time.[41]

$$S = \frac{\left(\frac{dm}{dt}\right)_{\max}\left(\frac{dm}{dt}\right)_{\min}}{T_{\mathrm{i}}^2 \times T_{\mathrm{b}}} \tag{6}$$

where $\left(\frac{dm}{dt}\right)_{max}$ is the maximum combustion rate (%/min), $\left(\frac{dm}{dt}\right)_{min}$ is the mean combustion rate, and T_i and T_b is the ignition and burnout temperature (°C).[42]

3 | RESULTS AND DISCUSSION

3.1 | Elements on the surface of raw samples

Identifying the elements bound to the raw samples is indispensable, as this has implications for their application as solid fuel and consequent environmental impact. The major elements detected on the surface of the dried raw samples by EDS analysis are shown in Figures 2–4.

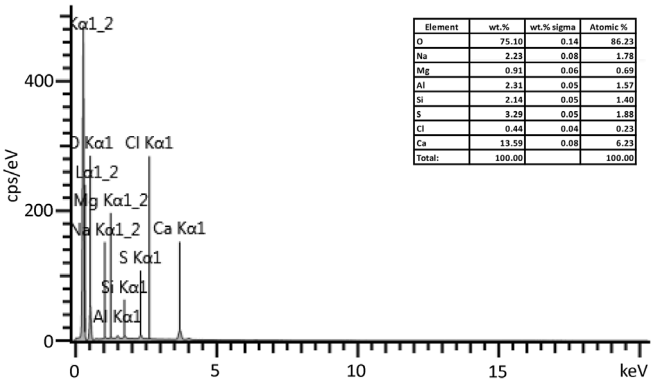

Element	wt.%	wt.% sigma	Atomic %
O	75.10	0.14	86.23
Na	2.23	0.08	1.78
Mg	0.91	0.06	0.69
Al	2.31	0.05	1.57
Si	2.14	0.05	1.40
S	3.29	0.05	1.88
Cl	0.44	0.04	0.23
Ca	13.59	0.08	6.23
Total:	100.00		100.00

FIGURE 2 Elemental composition of dried raw fibre rejects (RF) from energy-dispersed X-ray spectroscopy (EDS)

The EDS spectrum indicates that all samples consisted mainly of oxygen and calcium, with relatively small percentages of sulphur, aluminium, silicon, and traces of chlorine. Other minor elements, such as sodium and magnesium, were also detected on raw fibre sludge (RS) and final sludge (FS) samples, while traces of iron were detected on FS and PS samples. These elements contribute to the impurity of the raw feedstock and further affect the ash composition of the corresponding hydrochar.

3.2 | Energy properties of the hydrochars

The reaction mechanisms of hydrochar formation through the HTC process are mainly affected by temperature.[43] Increased temperature promotes devolatilization and dehydration, which consequently lowers the hydrochar yield and leads to a solid product with distinctive energy properties from its initial sample. Figures 5–7 depicts the energy properties of the raw samples and corresponding hydrochar at various temperatures. In contrast to the HHV and energy densification, the mass and energy yield declined as the carbonization temperature increased. This is due to hydrothermal degradation of the primary organic components found in the raw sludge such as cellulose, hemicellulose, and lignin.[27] The reactivity of the samples increased with temperature and, consequently, hydrochar with increased energy densification and higher HHV was obtained.

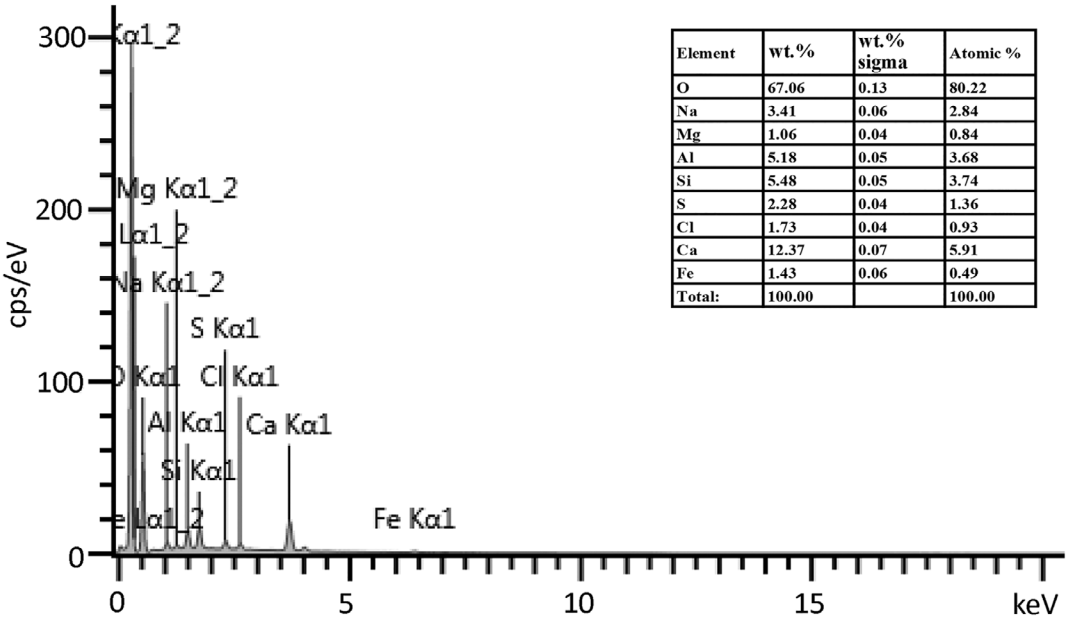

Element	wt.%	wt.% sigma	Atomic %
O	67.06	0.13	80.22
Na	3.41	0.06	2.84
Mg	1.06	0.04	0.84
Al	5.18	0.05	3.68
Si	5.48	0.05	3.74
S	2.28	0.04	1.36
Cl	1.73	0.04	0.93
Ca	12.37	0.07	5.91
Fe	1.43	0.06	0.49
Total:	100.00		100.00

FIGURE 3 Elemental composition of dried final waste sludge (FS) from energy dispersed X-ray spectroscopy (EDS)

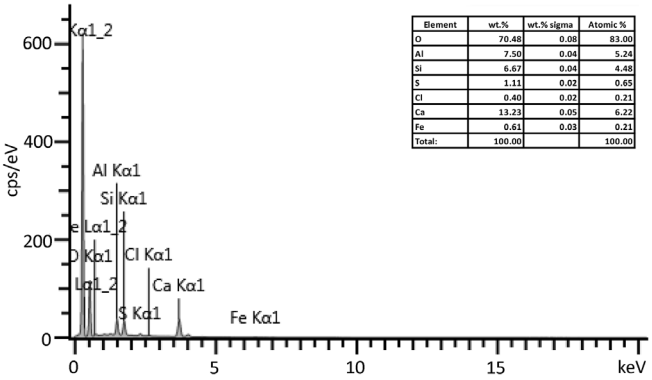

FIGURE 4 Elemental composition of primary clarifier sludge (PS) from energy dispersed X-ray spectroscopy (EDS)

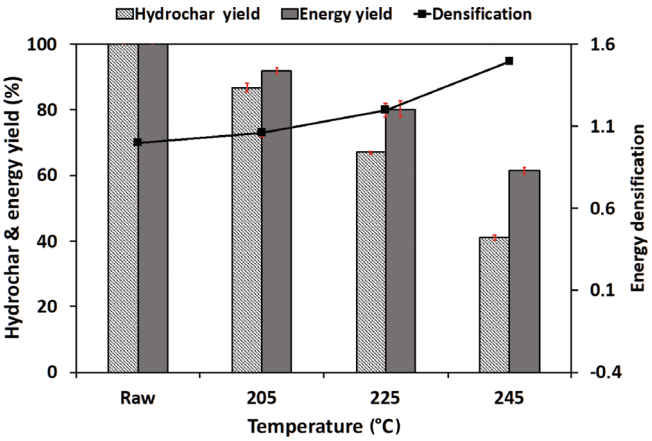

FIGURE 5 Effect of hydrothermal carbonization (HTC) temperature on hydrochar yield, energy yield, and energy densification of raw fibre rejects (RF) feedstock

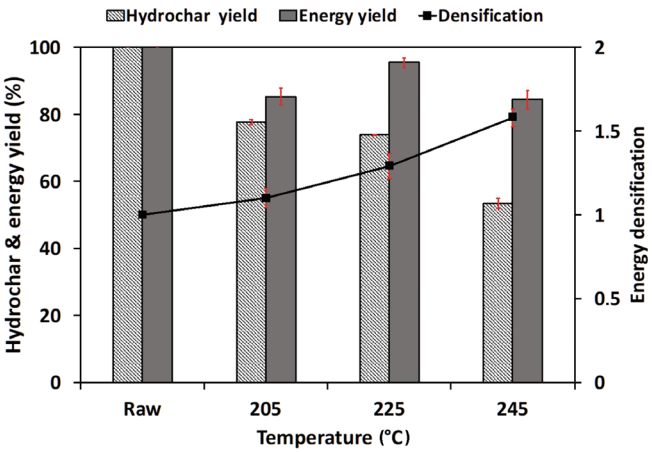

FIGURE 6 Effect of hydrothermal carbonization (HTC) temperature on hydrochar yield, energy yield, and energy densification of final waste sludge (FS) feedstock

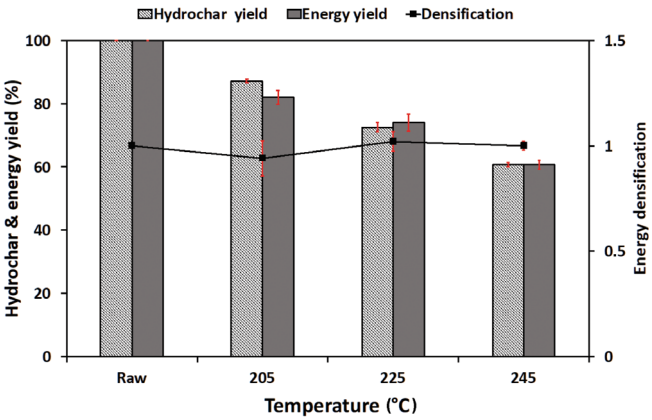

FIGURE 7 Effect of hydrothermal carbonization (HTC) temperature on hydrochar yield, energy yield, and energy densification of primary sludge (PS) feedstock

The HHV for RF and FS hydrochar ranged from 18.62–26.24 and 19.08–26.47 MJ/kg on a dry ash-free basis (daf), respectively, representing an increase of 5.98%–49.35% and 10.10%–58.51%. At 225–245°C, the HHV of RF and FS hydrochar was higher than 20 MJ/kg, which is comparable to coal used for commercial utility in South Africa.[4] In contrast, HTC had no significant effect on the energy densification and HHV of PS hydrochar. This could be due to the significant increase in ash content retained in the hydrochar as reaction temperature increased. The HHV for PS hydrochar varied from 13.27–14.33 MJ/kg and presented a decrease of 5.48% at 205°C compared to the raw samples. For energetic applications, fuels with relatively higher HHV are preferred.

3.3 | Chemical composition

The results of the elemental composition determined on a daf are illustrated in Figure 8. It is evident from the results that the chemical composition of the samples has undergone a significant change after HTC treatment. With the increase in reaction temperature, the carbon content of RS and FS samples significantly increased with a simultaneous decrease in oxygen content. This is due to dehydration and decarboxylation reactions, in which hydroxyl and carbonyl groups are reduced in the form of H_2O and CO_2.[44] Higher reaction severities accelerate the rate of devolatilization and lead to the continuous reduction of volatile matter.[21]

In terms of carbon fraction, the content for RF, FS, and PS hydrochar ranged from 45.18%–60.30%, 47.18%–83.75%, and 40.94%–48.63%, respectively. The highest carbon content present in the hydrochar was attained at 245°C, equivalent to an increase of 32.21%, 87.12%, and

THE CANADIAN JOURNAL OF CHEMICAL ENGINEERING

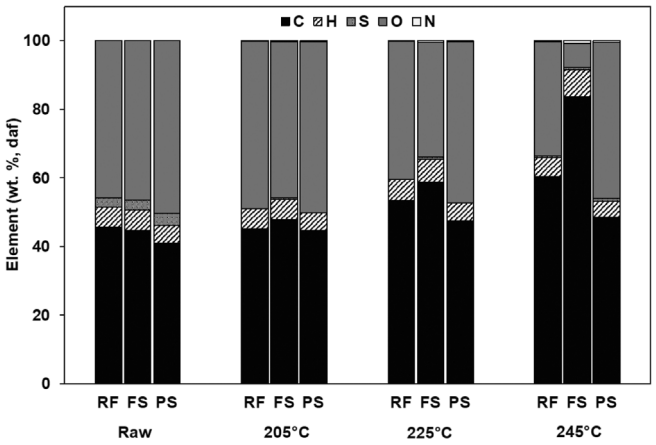

FIGURE 8 C, H, O, N, and S content of raw fibre rejects (RF), final waste sludge (FS), and primary sludge (PS) and hydrochar at different reaction temperatures on a dry ash-free basis (daf)

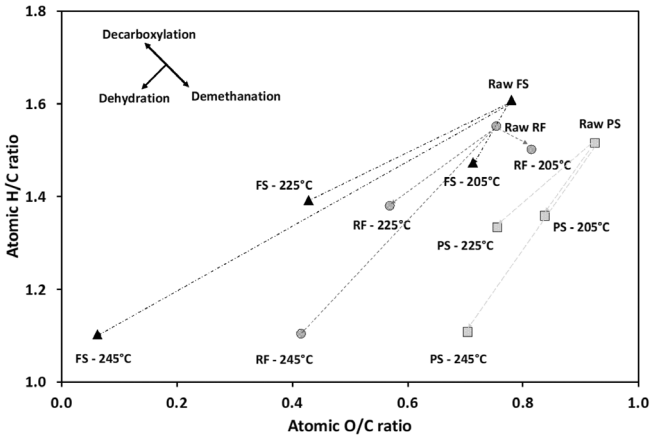

FIGURE 9 Van Krevelen diagram of raw fibre rejects (RF), final waste sludge (FS), and primary sludge (PS) and corresponding hydrochar at different reaction temperatures

18.78% for RF, FS, and PS, respectively. The oxygen content decreased by 27.22%, 85.03%, and 9.54% for RF, FS, and PS, respectively. A higher proportion of carbon and a lower percentage of oxygen have a positive influence on the calorific value of the solid fuel. These results are consistent with the energy properties reported in Section 3.2. The hydrogen content was unaffected by the reaction temperature, however, the overall H/C ratios decreased.

Furthermore, the nitrogen (N) and sulphur (S) contents of hydrochar are crucial properties to consider for fuel use. Generally, little to no sulphur and nitrogen fuel is preferred since these properties mitigate emissions of NO_x and SO_x during the combustion process. Although the nitrogen composition slightly increased with reaction temperature, it remained relatively low in all samples (less than 1%). The HTC reaction was also effective in reducing the sulphur content. This is due to the formation of sulphur oxides, which are consequently dissolved in the process water and, as a result, all hydrochars formed reported sulphur percentage much lower than their initial samples. These findings are consistent with previous research.[21,27] These characteristics indicate that HTC could be environmentally friendly to convert paper wastes into clean, high-value solid fuel with minimal nitrogen and sulphur composition.

3.4 | Fuel properties of the hydrochars

The relationship between the atomic H/C and O/C ratios, estimated from C, H, and O composition, was examined using the Van Krevelen diagram, as shown in Figure 9, to explore the coalification degree, conversion pathways involved in the HTC of paper sludge, and the fuel properties of the samples. The atomic H/C and O/C ratios of the hydrochar from the three substrates decreased as carbonization temperature increased, and the ratios were considerably lower than their initial feedstock, especially at 245°C where the H/C decreased by 29.03%, 31.62%, and 26.97% for RF, RS, and PS, respectively. Similarly, the O/C atomic ratio decreased by 44.00%, 92.31%, and 23.91% for RF, RS, and PS, respectively. This trend confirms that dehydration and decarboxylation reactions were dominant pathways for all reaction conditions, except for RF at 205°C, which, according to the coalification diagram, may have undergone demethanation. For fuel applications, low H/C and O/C atomic ratios are desired due to decreased smoke, water vapour, and energy losses during combustion.[45] These findings further suggest the improvement of hydrochar solid fuel as a result of HTC.

3.5 | Surface morphology

The microstructural changes of the hydrochar from RF, FS, and PS as a consequence of HTC are depicted in Figure 10. The morphology of the raw fibres consists of a long flat structure and a mostly smooth surface, as reported in the previous study.[39] The images in Figure 10 demonstrate the variation in structure with the increase in reaction temperature. For all samples, at 205°C, the hydrochar retained the fibrous structure with minimal degradation. At 225°C, it is possible to observe micro-fissures in the hydrochar, turning the structure rougher and more irregular. At 245°C, the hydrochar exhibited microstructural fragmentation and formation, agglomerated particles, and porous features. These observations confirm the degradation of organic components, particularly cellulose and hemicellulose, occurred as a result of thermochemical conversion reactions.[37,46] Furthermore, the improved porosity property characteristic of the hydrochar enhances its

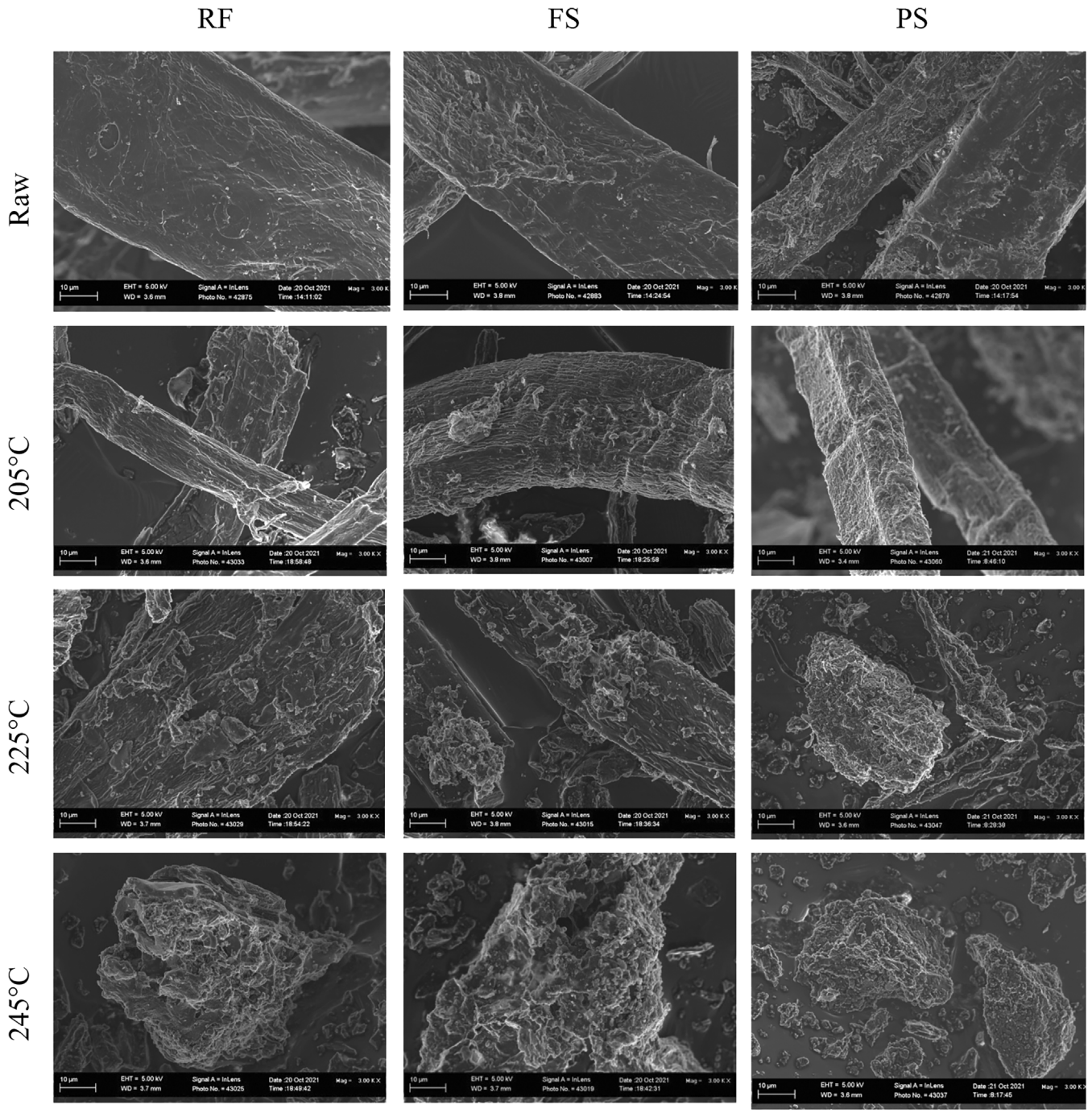

FIGURE 10 Scanning electron microscopy (SEM) images of raw fibre rejects (RF), final waste sludge (FS), and primary sludge (PS) hydrochar at different hydrothermal carbonization (HTC) temperatures

thermal reactivity during combustion by facilitating air access and distribution.

3.6 | Changes in functional groups of paper sludge-derived hydrochars

FTIR effectively characterizes the variation of functional groups in the samples and can further provide reference for further identification of the reaction mechanisms that occurred during the HTC process. The structures of the raw feedstocks and hydrochar spectra are shown in Figures 11–13. The difference in peak shapes indicates that although the three samples originate from recycling paper mill waste streams, they vary in chemical characteristics due to the source of fibre and process employed for pulp manufacturing and wastewater treatment. The bands at 3693 and 3621 cm^{-1} in the PS samples could be associated with the presence of kaolinite,[47] which, according to the observations, remained inert during HTC treatment.

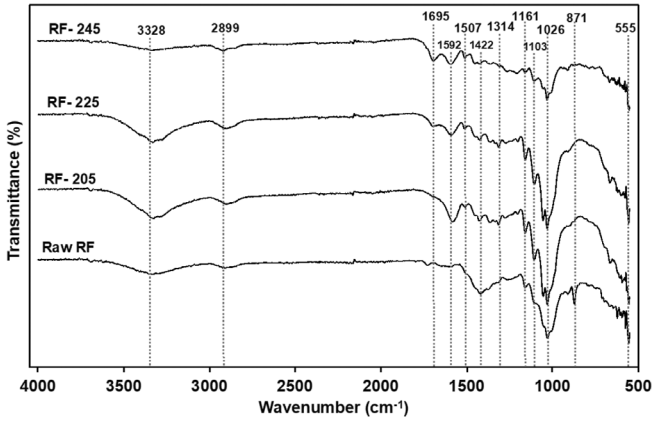

FIGURE 11 Fourier-transform infrared spectroscopy (FTIR) spectra of raw fibre rejects (RF) and hydrochars

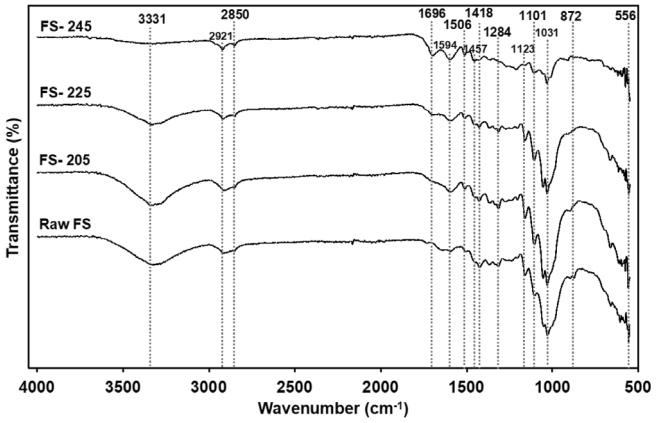

FIGURE 12 Fourier-transform infrared spectroscopy (FTIR) spectra of raw final waste sludge (FS) and hydrochars

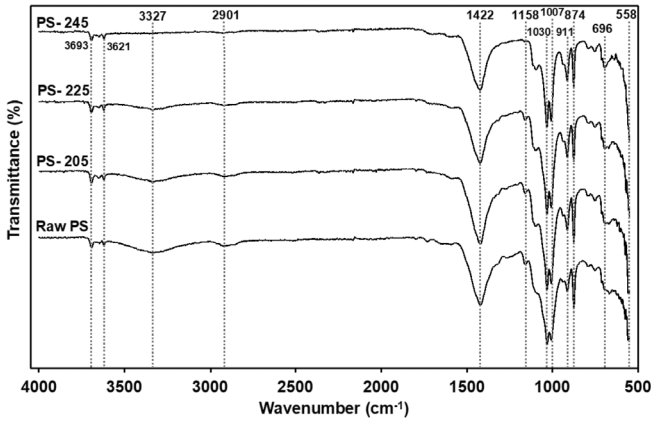

FIGURE 13 Fourier-transform infrared spectroscopy (FTIR) spectra of raw primary sludge (PS) and hydrochars

The absorption peaks at 3328, 3321, and 3327 cm^{-1} (between 3200 and 3650 cm^{-1}) mainly reflect the O—H stretching vibration from carboxyl or hydroxyl groups of phenolic structures, alcohols, and carboxylic acids[48]; the bands were less pronounced at HTC-245°C, confirming the occurrence of dehydration reaction during the HTC process.

The absorption peak at 2899 and 2901 cm^{-1} (between 2500 and 3200 cm^{-1}) for RF and PS samples are mainly caused by aliphatic C—H bonds from alkyl groups.[49] The peaks at 2921 and 2850 cm^{-1} for FS samples are associated with C—H symmetric and asymmetric stretching in —CH_2 and —CH_3 groups[48]; these peaks become less evident at higher temperatures, which suggests demethylation reaction occurred and was more pronounced at 245°C.

Regarding the 1500–2000 cm^{-1} range, the peaks at 1504–1506 cm^{-1} and 1592–1594 cm^{-1} for RF and FS correspond to C═C in-plane aromatic vibration.[50,51] The bands became more evident with an increase in HTC reaction temperatures and are more pronounced for RF-225°C and RF-245°C. This trend suggests the occurrence of aromatization reaction during the HTC process. The absorbance peaks at 1695 and 1696 cm^{-1} attributed to C═O stretching in ester groups,[51] and it is due to further dehydration and decarboxylation products formed and retained in the hydrochar[49]; this observation is more prominent at HTC-245°C for RF and FS hydrochars. This indicates that, under this condition, the chemical components of RF underwent simultaneous degradation and polymerization reaction.[30]

As for the range of 1300–1500 cm^{-1}, the peaks at 1314, 1418–1422 cm^{-1}, and 14 577 cm^{-1} for RF and FS could be due to —CH_2 rocking, —CH_2 scissoring, and O—H in-plane deformation, respectively.[52] The peaks at 1422 and 874 observed in PS samples are associated with elevated calcium carbonate content in the sample,[47,53] which remained unreactive during HTC. The change in peak intensity with the variation of reaction temperature indicates that HTC treatment had a significant impact on the functional groups of the derived hydrochars, particularly, RF and FS hydrochar samples. The organic matter at bands in the region of 1000–550 cm^{-1} could be attributed to single bond-stretching vibration frequencies as well as frequencies in the molecular skeleton[50] such as C—O and ring stretching, —CH_2 rocking, OH out-of-plane bending, as reported by Abidi et al.[52] The vibrations could also be attributed to anti-symmetrical bridge C—O—C in polysaccharides,[33] C—O stretching in carboxyl and/or carbonyl groups, β-linkage of cellulose and hemicellulose, C—H angular deformation in aromatic and alkyne groups, and O-H angular deformation in R—OH groups.[33,51,52] This confirms the presence of polysaccharides from lignocellulose structure and the occurrence of dehydration, decarboxylation, and aromatization reactions during HTC.[36,54] In the same region, the intensity peaks showed no obvious change for PS hydrochars with the increase in reaction temperature.

This is because PS feedstocks contain elevated amounts of $CaCO_3$, which is typically used as a filler and pigment to brighten the produced paper.[55] These results confirm that HTC treatment had no influence on the degradation of inorganic components, including $CaCO_3$. Unlike RF and FS hydrochars, HTC had little effect on the overall surface properties of PS hydrochars.

The observations from this analysis confirm that dehydration and decarboxylation reactions govern the hydrochar formation, especially for RF and FS samples at 245°C. Moreover, polymerization and aromatization reactions occurred to some degree.

3.7 | Combustion characteristics

3.7.1 | Weight loss and derivative weight profiles

The evaluation of combustion performance is crucial to determine the suitability of fuel for heat conversion through incineration. Optimum combustion performance is characterized by reduced fuel consumption and costs.[21] The TG profiles of the raw samples and hydrochar at different reaction temperatures, measured at between 50 and 950°C at 20°C/min, as well as the corresponding DTG, are illustrated in Figures 14–16 to clarify the different combustion stages with the corresponding weight losses. The units are expressed in %/°C. For better evaluation of the combustion behaviour of the samples, the TG-DTG profiles were divided into four stages. The first stage is dehydration, which occurred below 200°C and corresponds to the removal of residual moisture. The second stage, which occurred between 200 and 400°C, is attributed to the combustion of volatile organic matter such as cellulose and hemicellulose, as well as the partial decomposition of lignin. The third stage, which occurred between 400 and 600°C, is related to char combustion, which is associated with lignin decomposition. Lastly, the fourth stage, which occurred at temperatures higher than 600°C, is associated with volatile inorganic decomposition, and is considered the burnout stage.

The variation of the HTC reaction temperatures resulted in hydrochar with a TG-DTG pattern

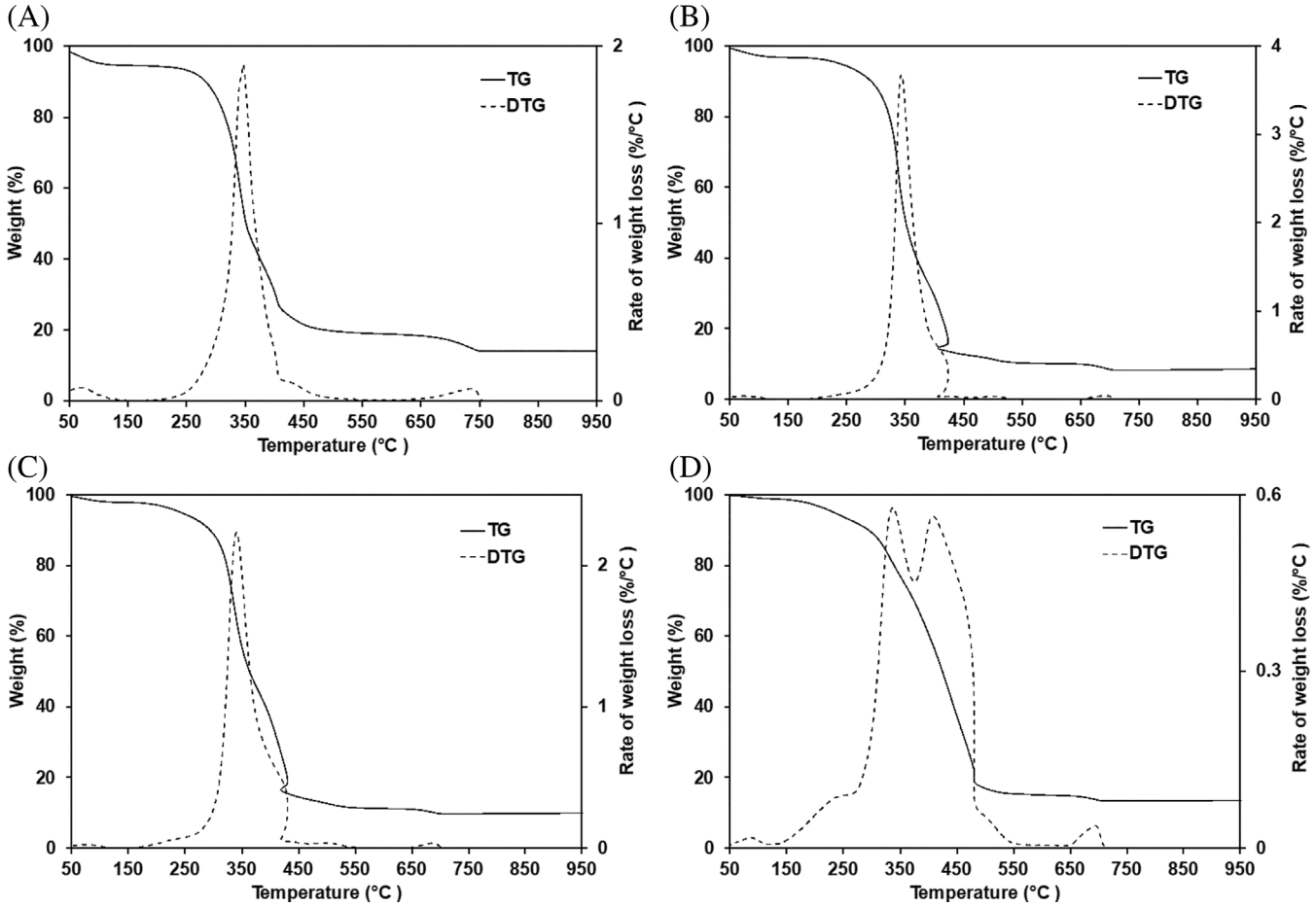

FIGURE 14 Thermogravimetry-derivative thermogravimetry (TG-DTG) profiles of (A) raw fibre rejects (RF) and hydrochar obtained at (B) 205°C, (C) 225°C, and (D) 245°C

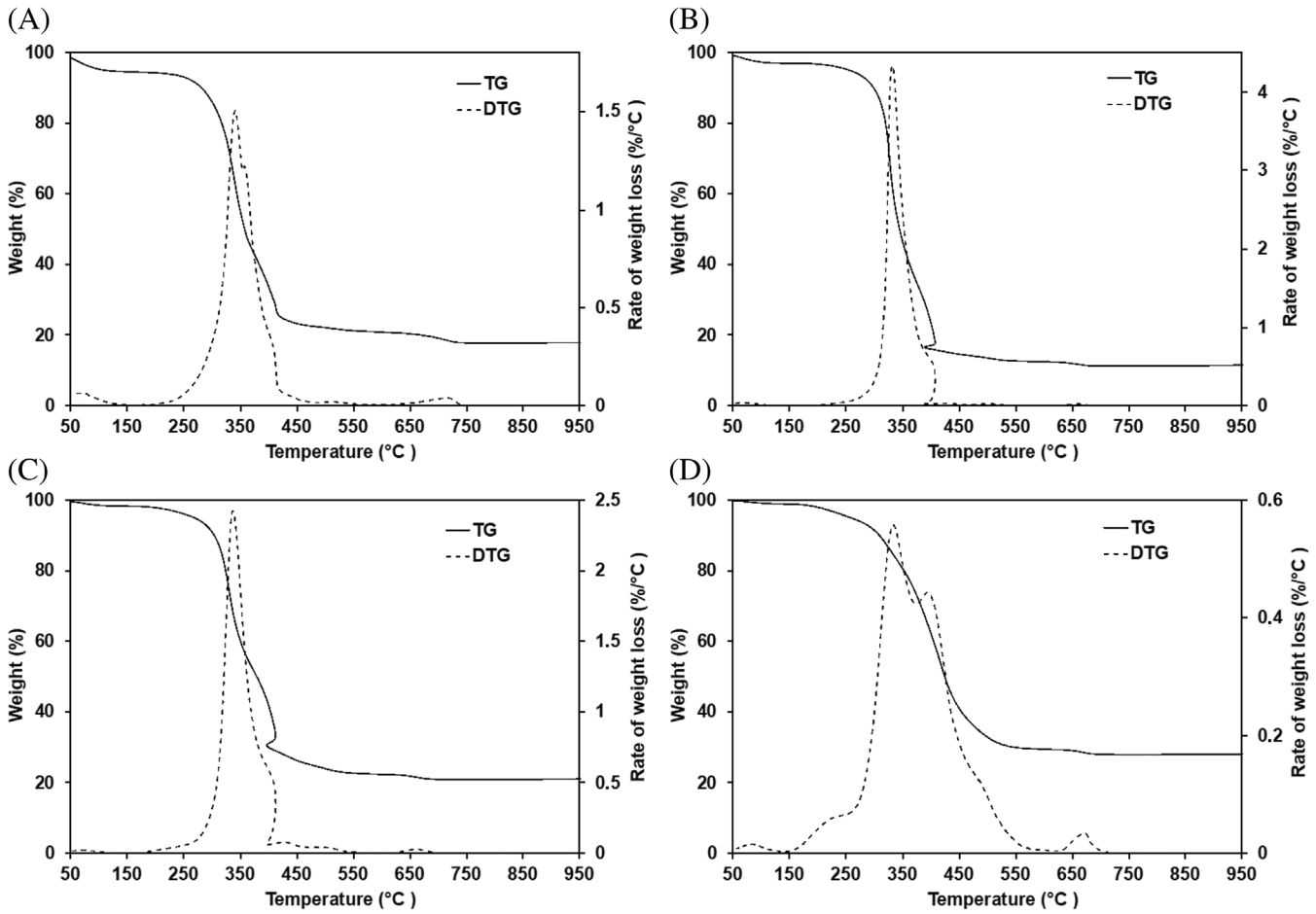

FIGURE 15 Thermogravimetry-derivative thermogravimetry (TG-DTG) profiles of (A) raw final waste sludge (FS) and hydrochar obtained at (B) 205°C, (C) 225°C, and (D) 245°C

distinctive from that of the raw feedstock, especially for hydrochar obtained at 205 and 225°C. At this temperature range, the rate of mass loss increased dramatically, and this observation is more pronounced at 205°C where the $(dm/dt)_{max}$ increased from 1.90% to 3.78%/°C, 1.51% to 4.34%/°C, and from 1.39% to 1.88%/°C for RF, FS, and PS, respectively. In contrast, the maximum rate of mass loss decreased drastically at 245°C, reaching values of 0.56%/°C, 0.51%/°C, and 0.26%/°C for RF, FS, and PS, respectively. Moreover, the corresponding temperature (T_m) was relatively lower than that of the raw samples. This could be because, during the HTC, the substrates decomposed into products with simpler chemical structures and higher reactivity compared to the raw samples.[27] Thus, during the combustion process, the chemical bonds of these samples are easily broken, resulting in an increased rate of combustion. The reduced mass loss rate at 245°C is attributed to the decreased volatile content in the form of cellulose and hemicellulose, which almost completely decompose as the temperature approaches 250°C,[37] it is also due to the increased fixed carbon in the form of lignin, which has higher thermal stability.[56] Furthermore, the peaks in the range of 385–512°C became more pronounced for hydrochar obtained at 245°C, especially for RF. This implies that more fixed carbon was generated with an increase in HTC reaction temperature. High fixed carbon and low volatile matter content translate to better combustion performance due to reduced vigorous and a more stable flame.[57]

3.7.2 | Ignition temperature

The ignition temperature determines how easily a given fuel is ignited, and the combustion parameters are summarized in Table 1. The values observed were in the range of 294.96–316.53°C, 292.30–315.05°C, and 309.00–314.57°C, for RF, RF, and PS, respectively. A similar range was observed by Gao et al.[58] and Lin et al.[27] for agricultural

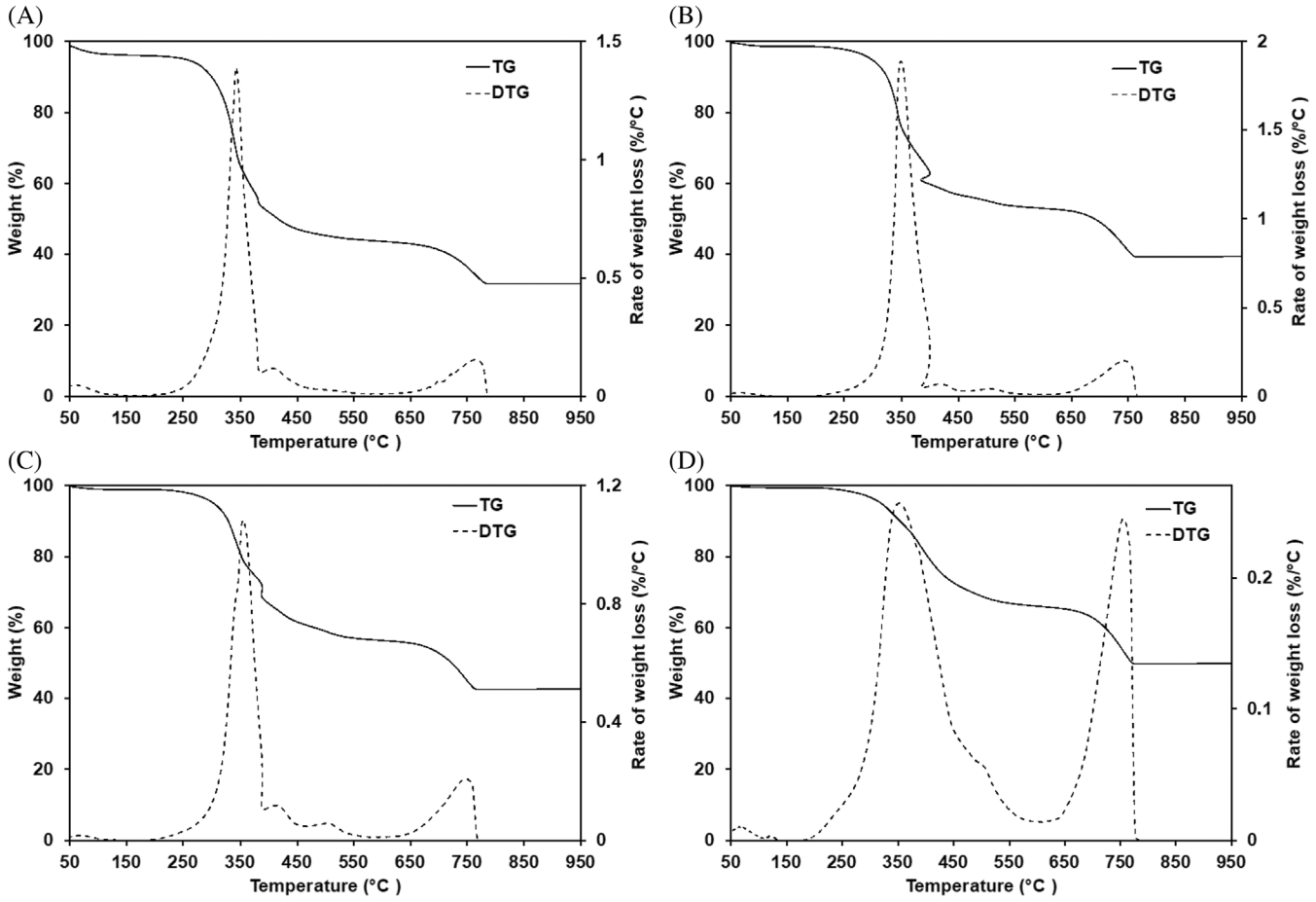

FIGURE 16 Thermogravimetry-derivative thermogravimetry (TG-DTG) profiles of (A) raw primary sludge (PS) and hydrochar obtained at (B) 205°C, (C) 225°C, and (D) 245°C

TABLE 1 Combustion parameters of the raw samples and hydrochars

Sample	T_i (°C)	T_b (°C)	t_i (min)	T_{max} (°C)	$(dm/dt)_{max}$ (%/min)	D_i (%/min^3)	S (%^{2}/min^2 °C^3)
Raw RF	305.54	746.32	14.13	345.61	37.95	17.18E−02	8.12E−07
RF-205°C	316.53	705.60	15.59	343.00	73.91	29.03 E−02	16.94E−07
RF-225°C	307.22	697.36	15.05	340.87	44.98	18.66 E−02	11.00E−07
RF-245°C	294.96	703.32	14.38	337.32	11.23	4.57 E−02	2.85E−07
Raw FS	306.17	726.80	14.07	342.76	30.09	13.95 E−02	6.32E−07
FS-205°C	315.05	681.04	15.48	331.72	86.75	35.22 E−02	20.30E−07
FS-225°C	307.85	684.29	15.03	336.30	48.17	20.27 E−02	10.47E−07
FS-245°C	292.30	685.99	14.29	332.37	10.15	4.615 E−02	2.11 E−07
Raw PS	309.65	786.96	14.24	344.63	27.80	12.60 E−02	4.38E−07
PS-205°C	320.67	762.19	15.78	349.93	37.61	14.30 E−02	5.18E−07
PS-225°C	314.57	767.44	15.52	356.82	20.04	7.67 E−02	2.72E−07
PS-245°C	309.00	772.13	15.26	352.92	5.13	2.01 E−02	6.20E−08

Abbreviations: FS, final waste sludge; PS, primary sludge; RF, raw fibre rejects.

waste and paper sludge-derived hydrochar. All hydrochars obtained at HTC treatment of 205 and 225°C presented higher ignition temperatures compared to the raw substrates due to the decomposition of cellulose and hemicellulose.[59] This translated to a higher ignition index (D_i), which implies better combustion performance.

3.7.3 | Burnout temperature

The burnout temperature is an important fuel parameter. It indicates the maximum temperature at which the fuel is almost completely consumed during combustion.[40] The results of the burnout temperatures are also presented. Generally, fuels with high burnout temperatures require longer residence times and higher temperatures to achieve complete combustion. The increase in reaction temperatures led to reduced burnout temperatures. This is more pronounced for RF and FS at 245°C where a reduction of ~40°C was observed. The burnout temperature for PS was the least affected.

3.7.4 | Combustibility index

The calculated combustibility index (S) of the raw samples and corresponding hydrochar are given in Table 1. A higher S value suggests a more active combustion ability. Hydrochar produced at HTC treatment of 205 and 225°C presented S values greater than those of the raw samples due to the increased maximum weight loss rate. When comparing the samples, FS-205°C performed the best S value $20.3 \times 10^{-7}\%^2/\text{min}^2$. Those values were followed by $16.94 \times 10^{-7}\%^2/\text{min}^2$, $11.00 \times 10^{-7}\%^2/\text{min}^2$, and $10.47 \times 10^{-7}\%^2/\text{min}^2$ for RF-205, FS-225, and FS-225°C, respectively. These results suggest an improved combustion performance. Therefore, HTC is effective in producing hydrochar with enhanced combustion properties under appropriate reaction temperatures. When comparing the three substrates, PS samples presented the lowest combustion. This is attributed to the high burnout temperature resulting from the relatively low carbon content in the form of volatile matter and fixed carbon, as well as high inorganics in the initial substrate and derived hydrochar matrix. Under non-isothermal heating, these characteristics hinder complete combustion and efficient transportation of CO_2 and O_2 gas and require a longer time for complete burning[60]; thus, combustion occurs with difficulty.

3.7.5 | Residual ash

The ash content remained after the combustion of the raw samples and the hydrochar obtained at different HTC treatment temperatures is presented in Figure 17. The characteristics of the sludge depend on the source of cellulose, the employed process of production, and the final products produced at the mills' operations. RF residues were formed during the re-pulping process, FS solids were from the raw wastewater treatment prior to final disposal, and PS solids were formed during the physicochemical treatment of the wastewater at the primary clarifier where suspended solids, colloidal particles, floating matters, colours, and toxic compounds are removed by either sedimentation, flotation, screening, adsorption, coagulation, oxidation, ozonation, reverse osmosis, ultra-filtration, or nano-filtration techniques.[61] Due to the characteristics of the wastewater from the paper mill processes, the resulting solid residues (PS) contain higher inorganic fillers, including calcium carbonate and chemicals dissolved in water during pulping, paper making, and wastewater primary treatment. Results showed that residual ash composition changed significantly post HTC treatment. The residual ash composition varied from 9.56%–14.85%, 11.89%–28.50% and 33.00%, and 50%–26% for RF, FS, and PS, respectively. In general, PS hydrochar presented the highest residual ash composition post-combustion, especially at HTC-245°C where a value of 50.52% was observed. The utilization of fuel with high ash has negative implications for the environment and the technical design of a processing plant, as this requires further processing and disposal. Thus, based on these results, PS hydrochar is considered unfit for fuel application. RF hydrochar presented ash residues relatively lower than the raw substrates at all HTC temperatures. This could be because during HTC, the inorganic components present in the RF raw feedstock matrix are extracted and partially dissolved in the process water.[21,62] For solid fuel applications, low ash is preferred as it prevents problems that are associated with fouling, scaling, slagging, and corrosion in combustion chambers.

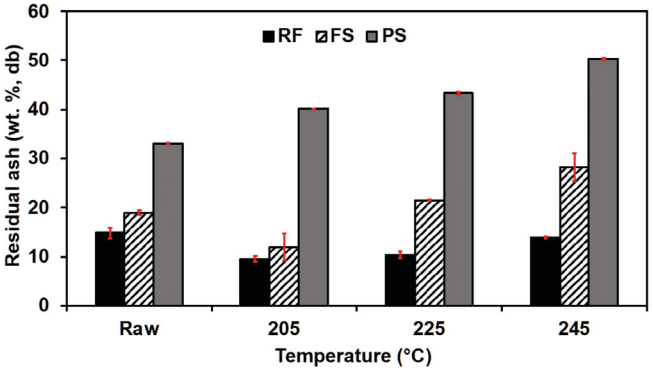

FIGURE 17 Residual ash of the raw samples and hydrochars post-combustion. FS, final waste sludge. PS, primary sludge. RF, raw fibre rejects

The results obtained in this research suggest that the HTC process could be an efficient technology to upgrade the underutilized paper waste into clean, high-value solid fuel with low contaminants. This is particularly true for RF and FS, as the derived hydrochars reported enhanced energy properties, improved chemical characteristics, surface morphology, and enhanced reactivity, which translated to a positive combustion performance. Thus, such

hydrochars could play a role in mono-combustion or co-combustion with coal at existing coal-fired power plants to generate energy in the form of heat or power.

4 | CONCLUSIONS

This research evaluated the effect of HTC temperature on the conversion mechanisms, physicochemical properties, and combustion behaviour involved in the hydrochar formation from RF, FS, and primary clarifier wastewater sludge from recycling paper mills, in relation to the raw feedstocks. The increment of reaction temperature led to a decrease in mass yield and an increase in the energy densification for RF and FS hydrochars, but no significant effect on the energy density of hydrochar derived from the primary clarifier. The calorific value of RF and FS increased by up to 49.35% and 58.51%, respectively. Dehydration and decarboxylation were the most predominant reaction mechanisms, which lowered the H/C and O/C ratios as the reaction temperature increased. The produced hydrochars presented low nitrogen and sulphur content, which validates the efficiency of the HTC treatment as an environmentally friendly technology to convert paper wastes into high-value clean solid fuel with improved thermal reactivity. RF-derived hydrochars exhibited better fuel properties due to the increased carbon content, HHV, combustion adequacy, and low ash content. Thus, the hydrochar obtained from these streams can play a role in the energy field as an alternative to coal or in co-combustion. Due to elevated ash retained in the hydrochar matrix and unchanged energy densification, PS was considered unfit for solid fuel applications.

In order to provide basis for the improvement in the rational utilization of hydrochar fuel on an industrial level and reduce over-reliance on coal to mitigate excessive carbon dioxide emissions, a study on the effect of co-combustion of paper waste-derived hydrochar and low-rank coal, that is, lignite, should be conducted for the potential to upgrade their rank by lowering the oxygen and moisture content. The high alkali metals in coal reduce the ash melting points, which represents a major drawback during incineration due to severe slagging and fouling on the heating surface of the incinerators. Thus, the effect of incineration of hydrochar-coal blends at different ratios and ashing temperatures on the ash yield and physicochemical characteristics of the post-combustion residuals should also be explored and compared with that of coal.

NOMENCLATURE

A	ash
daf	dry ash-free basis
db.	dry basis
D_i	ignition index
E_D	energy densification
E_Y	energy yield
FC	fixed carbon
FS	final sludge
GHG	greenhouse gases
HHV	higher heating value
HTC	hydrothermal carbonization
H_Y	hydrochar yield
M	moisture content
RF	raw fibre rejects
S	comprehensive combustibility index
T_b	burnout temperature
t_i	ignition time
T_i	ignition temperature
T_m	maximum combustion rate temperature
t_{max}	time at maximum combustion rate
VM	volatile matter

AUTHOR CONTRIBUTIONS

Englatina I. N. C. Assis: Conceptualization; data curation; formal analysis; investigation; methodology; project administration; writing – original draft. **Evans M. N. Chirwa:** Conceptualization; funding acquisition; resources; supervision; validation; writing – review and editing.

ACKNOWLEDGEMENTS

Research funding was provided by the Sedibeng Water Chair in Water Utilization Engineering (Grant No. 4540105923), Rand Water Chair in Water Utilization and National Research Foundation (NRF), Grant No. IFR200206501999, CSUR210111581519, and EQP210111581520, awarded to Professor Evans M.N. Chirwa of the Water Utilization and Environmental Engineering Division at the University of Pretoria.

CONFLICT OF INTEREST

The authors declare that they have no known competing financial interest or personal relationship that could have appeared to influence the work reported in this paper.

PEER REVIEW

The peer review history for this article is available at https://publons.com/publon/10.1002/cjce.24708.

DATA AVAILABILITY STATEMENT

The data that support the findings of this study are available from the corresponding author upon reasonable request.

REFERENCES

[1] N. S. Ouedraogo, *Energy Policy* **2017**, *106*, 457.
[2] Internation Energy Agency, http://energyatlas.iea.org/#!/tellmap/2020991907/0 (accessed: July 2022).

[3] S. Jain, P. K. Jain, *Energy Procedia* **2017**, *143*, 721.
[4] S. S. Makgato, E. M. Chirwa, *J. Environ. Manage.* **2017**, *201*, 294.
[5] O. M. Akinbami, S. R. Oke, M. O. Bodunrin, *Alexandria Eng. J.* **2021**, *60*(6), 5077.
[6] S. Boshoff, L. D. Gottumukkala, E. van Rensburg, J. Görgens, *Bioresour. Technol.* **2016**, *203*, 103.
[7] R. Kaur, R. D. Tyagi, X. Zhang, *Environ. Res.* **2020**, *182*, 109094.
[8] G. M. Scott, in *Int. Environmental Conf. Proc*. TAPPI Press, **1995**.
[9] P. Bajpai, *Management of Pulp and Paper Mill Waste*, Springer, Cham, Switzerland **2015**. https://doi.org/10.1007/978-3-319-11788-1
[10] M. Likon, P. Trebe, in *Industrial Waste* (Eds: K. Show, X. Guo), InTechOpen, London, UK **2012**, p. 73. https://doi.org/10.5772/37043
[11] F. Bergius, *Die Anwendung hoher drucke bei chemischen Vorgängen und eine nechbildung des Entstehungsprozesses der Steinkohle*, Wilhelm Knapp, Saale **1913**.
[12] A. Funke, F. Ziegler, *Biofuels, Bioprod. Biorefin.* **2010**, *4*(2), 160.
[13] Q. Wang, H. Li, L. Chen, X. Huang, *Carbon* **2001**, *39*(14), 2211.
[14] M.-M. Titirici, A. Thomas, M. Antonietti, *New J. Chem.* **2007**, *31*(6), 787.
[15] K. Kleiner, *Nat. Clim. Change* **2009**, *1*, 72.
[16] M. C. Rillig, M. Wagner, M. Salem, P. M. Antunes, C. George, H.-G. Ramke, *Applied Soil Ecology* **2010**, *45*, 238.
[17] K. S. Ro, J. Novak, S. Bae, J. R. V. Flora, N. D. Berge, presented at American Chemical Society National Meeting, San Francisco, CA, December **2010**.
[18] J. A. Libra, K. S. Ro, C. Kammann, A. Funke, N. D. Berge, Y. Neubauer, M.-M. Titirici, C. Fühner, O. Bens, J. Kern, K.-H. Emmerich, *Biofuels* **2011**, *2*(1), 71.
[19] M. Mäkelä, V. Benavente, A. Fullana, *Appl. Energy* **2015**, *155*, 576.
[20] V. Mau, J. Quance, R. Posmanik, A. Gross, *Bioresour. Technol.* **2016**, *219*, 632.
[21] W. Liang, G. Wang, R. Xu, X. Ning, J. Zhang, X. Guo, L. Ye, J. Li, C. Jiang, P. Wang, C. Wang, *Energy* **2022**, *246*, 123343.
[22] Q. Lang, Z. Liu, Y. Li, J. Xu, J. Li, B. Liu, Q. J. Sun, *J. Environ. Chem. Eng.* **2022**, *10*(1), 106938.
[23] I. S. Mohammed, R. Na, K. Kushima, N. Shimizu, *Sustainability* **2020**, *12*(12), 5100.
[24] Z. Li, W. Yi, Z. Li, C. Tian, P. Fu, Y. Zhang, L. Zhou, J. Teng, *Energies* **2020**, *13*(2), 480.
[25] E. Danso-Boateng, R. G. Holdich, S. J. Martin, G. Shama, A. D. Wheatley, *Energy Convers. Manage.* **2015**, *105*, 1115.
[26] M. Wilk, M. Śliz, M. Gajek, *Renewable Energy* **2021**, *177*, 216.
[27] Y. Lin, X. Ma, X. Peng, S. Hu, Z. Yu, S. Fang, *Appl. Therm. Eng.* **2015**, *91*, 574.
[28] D. Basso, D. Castello, M. Baratieri, L. Fiori in *21st European Biomass Conf. and Exhibition*, University of Trento, Copenhagen **2013**.
[29] W. Yan, S. K. Hoekman, A. Broch, C. J. Coronella, *Environ. Prog. Sustainable Energy* **2014**, *33*(3), 676.
[30] S. Guo, X. Dong, K. Liu, H. Yu, C. Zhu, *BioResources* **2015**, *10*(3), 4613.
[31] M. Heidari, A. Dutta, B. Acharya, S. Mahmud, *J. Energy Inst.* **2019**, *92*(6), 1779.
[32] R. Y. Spitzer, V. Mau, A. Gross, *J. Cleaner Prod.* **2018**, *205*, 955.
[33] M. Śliz, M. Wilk, *Renewable Energy* **2020**, *156*, 942.
[34] T. Wang, Y. Zhai, Y. Zhu, C. Li, G. Zeng, *Renewable Sustainable Energy Rev.* **2018**, *90*, 223.
[35] E. I. Assis, E. M. Chirwa, S. M. Tichapondwa, *Chemical Engineering Transaction* **2021**, *88*, 43.
[36] D. Kim, S. Park, K. Y. Park, *Energy* **2017**, *141*, 598.
[37] L.-P. Xiao, Z.-J. Shi, F. Xu, R.-C. Sun, *Bioresour. Technol.* **2012**, *118*, 619.
[38] W. Kirmse, *Organic Elemental Analysis: Ultramicro, Micro, and Trace Methods*, Elsevier, London, UK **2012**.
[39] E. I. Assis, E. M. Chirwa, *Chemical Engineering Transaction* **2021**, *86*, 607.
[40] J.-J. Lu, W.-H. Chen, *Appl. Energy* **2015**, *160*, 49.
[41] X.-G. Li, B.-G. Ma, L. Xu, Z.-W. Hu, X.-G. Wang, *Thermochim. Acta* **2006**, *441*(1), 79.
[42] Y. Lin, X. Ma, X. Ning, Z. Yu, *Energy Convers. Manage.* **2015**, *89*, 727.
[43] R. Sharma, K. Jasrotia, N. Singh, P. Ghosh, S. Srivastava, N. R. Sharma, J. Singh, R. Kanwar, A. Kumar, *Chem. Afr.* **2020**, *3*, 979.
[44] J. Fang, L. Zhan, Y. S. Ok, B. Gao, *J. Ind. Eng. Chem.* **2018**, *57*, 15.
[45] H. S. Kambo, A. Dutta, *Appl. Energy* **2014**, *135*, 182.
[46] C. Gai, Y. Guo, T. Liu, N. Peng, Z. Liu, *Int. J. Hydrogen Energy* **2016**, *41*(5), 3363.
[47] A. Méndez, J. M. Fidalgo, F. Guerrero, G. Gascó, *J. Anal. Appl. Pyrolysis* **2009**, *86*(1), 66.
[48] J. V. Santos, L. G. Fregolente, M. J. Laranja, A. B. Moreira, O. P. Ferreira, M. C. Bisinoti, *Biomass Convers. Biorefin.* **2021**, *12*, 153.
[49] N. Saha, A. Saba, M. T. Reza, *J. Anal. Appl. Pyrolysis* **2019**, *137*, 138.
[50] X. Li, Y. Wei, J. Xu, N. Xu, Y. He, *Biotechnol. Biofuels* **2018**, *11*, 263.
[51] J. Coates, *Encyclopedia of Analytical Chemistry: Applications, Theory and Instrumentation*, Wiley, Chichester, UK **2006**.
[52] N. Abidi, L. Cabrales, C. H. Haigler, *Carbohydr. Polym.* **2014**, *100*, 9.
[53] T. Thriveni, J. Whan Ahn, C. Ramakrisna, *J. MMIJ* **2017**, *133*(1), 1.
[54] J. Liu, S. Zhang, C. Jin, K. E. Sheng, X. Zhang, *ACS Sustainable Chem. Eng.* **2019**, *7*(12), 10821.
[55] L. J. Brown, F.-X. Collard, J. Görgens, *Energy Convers. Manage.* **2017**, *133*, 110.
[56] S. Kang, X. Li, J. Fan, J. Chang, *Renewable Sustainable Energy Rev.* **2013**, *27*, 546.
[57] X. Chen, X. Ma, X. Peng, Y. Lin, Z. Yao, *Bioresour. Technol.* **2018**, *249*, 900.
[58] W. Gao, X.-H. Wang, H.-P. Yang, H.-P. Chen, *Energy* **2012**, *42*(1), 457.
[59] F. Restuccia, O. Mašek, R. M. Hadden, G. Rein, *Fuel* **2019**, *236*, 201.
[60] S. Aich, D. Behera, B. K. Nandi, S. Bhattacharya, *Int. J. Coal Sci. Technol.* **2020**, *7*(4), 766.
[61] D. Pokhrel, T. Viraraghavan, *Sci. Total Environ.* **2004**, *333*(1–3), 37.
[62] L. J. Hansen, S. Fendt, H. Spliethoff, *Biomass Convers. Biorefin.* **2022**, *12*(7), 2541.

How to cite this article: E. I. N. C. Assis, E. M. N. Chirwa, *Can. J. Chem. Eng.* **2023**, *101*(3), 1123. https://doi.org/10.1002/cjce.24708